Nonlinear frequency shift caused by asymmetry of the multipeak coherent population trapping resonance

E. A. Tsygankov,* D. S. Chuchelov, M. I. Vaskovskaya, V. V. Vassiliev, S. A. Zibrov, and V. L. Velichansky
Laboratory of Frequency Standards, P. N. Lebedev Physical Institute of the Russian Academy of Sciences, Leninsky Prospect 53, Moscow 119991, Russia

(Received 2 February 2024; accepted 5 April 2024; published 2 May 2024)

We study the coherent population trapping resonance induced by the radiation of a microwave-current-modulated diode laser. The situation is considered when a harmonic phase modulation of the microwave field is used to generate the error signal for the frequency stabilization of atomic clocks. We demonstrate that in this case the resonance acquires a multipeak structure. If it is asymmetric and the components of the multipeak structure are not fully resolved, then the resonance frequency nonlinearly depends on the laser field intensity. The peaks become separated at an increase in the frequency of the phase modulation, providing a linear dependence of the frequency on the intensity of the laser field. This theoretical prediction is confirmed experimentally. Other advantages of the high-frequency modulation regime are also discussed.

DOI: 10.1103/PhysRevA.109.053703

I. INTRODUCTION

The coherent population trapping (CPT) phenomenon has been widely used to develop chip-scale atomic clocks [1]. Small size and low-power consumption are the main advantages of CPT clocks that make them attractive for many applications. The main elements of these devices are a vertical-cavity surface-emitting laser and a miniature glass cell filled with alkali-metal atoms and a buffer gas [2,3]. A microwave modulation of the laser's injection current is used to obtain a required optical field to induce the CPT resonance. Typically, the modulation frequency Ω is equal to the half of the alkali-metal atoms' ground-state hyperfine splitting ω_g. In this case the first sidebands of the laser field (often called "resonant components") are tuned to the absorption line. The transmission signal depends on the difference $2\Omega - \omega_g = \delta$ and reaches its maximum level at $\delta = 0$.

To stabilize the local oscillator frequency at the peak of the CPT resonance, the frequency Ω or its phase can be harmonically modulated ($\Omega \to \Omega + m\,\omega_m \cos \omega_m t$, where m is the phase modulation index), which provides oscillations of the light absorption at multiples of ω_m. The oscillation signals $\propto \cos \omega_m t$ and $\propto \sin \omega_m t$ are called in-phase and quadrature signals, respectively. The mixture of these signals, which has a dispersive shape and provides maximum slope, is often taken as an error signal [4,5].

The light shift of the CPT resonance frequency is considered to be the main factor limiting the long-term frequency stability of CPT clocks [6–10]. The standard approach to its suppression in the case of chip-scale devices is to find a specific optical spectrum for which the light shift caused by high-order sidebands ($k \geqslant 2$, where k is the spectral component number) compensates for the shift caused by the carrier and resonant components [11–13] (this is possible if the buffer gas pressure is not too high [14]).

In most cases, the first-order sidebands have unequal powers due to a nonlinear interaction of spectral components in the active medium of the diode laser [15], which leads to the asymmetry of the CPT resonance. In Ref. [16] we have obtained analytical expressions for the frequency shift δ_{as} of the zero-crossing point of in-phase and quadrature signals occurring due to the resonance asymmetry. It was shown that this shift has a nonlinear dependence on the laser field intensity in contrast to the light shift. Later this result was also obtained in Ref. [17]. This feature hinders the effectiveness of techniques for the suppression of the microwave transition frequency's light shift based on modulation of the total optical field intensity in the following way. When the condition $\partial(\delta_{as} + \delta_0)/\partial I = 0$ is fulfilled, where δ_0 is the light shift, the total shift is not equal to zero, $\delta_{as} + \delta_0 \neq 0$. Then, despite the fact that the zero of the error signal does not respond to variations in the optical field intensity, the corresponding frequency still remains shifted from the frequency of the microwave transition. The value of this shift depends on the degree of the CPT resonance's asymmetry, which is determined by the parameters of the laser radiation and the atomic medium. Therefore, the clock frequency can undergo random walks which reduce the clocks' performance.

In this paper, we demonstrate that a nonlinear dependence of δ_{as} on the laser field intensity stems from a multipeak structure of the resonance, wherein the distance between peaks is determined by the frequency ω_m. Therefore, the frequency of the central peak is pulled by other peaks in the case of an unresolved structure. We experimentally demonstrate that suppression of the frequency pulling at high values of ω_m provides a linear dependence of δ_{as} on I, which was proposed in Ref. [17].

II. THEORY

To describe the coherent population trapping resonance, at least a Λ system of levels is required. The

*tsygankov.e.a@yandex.ru

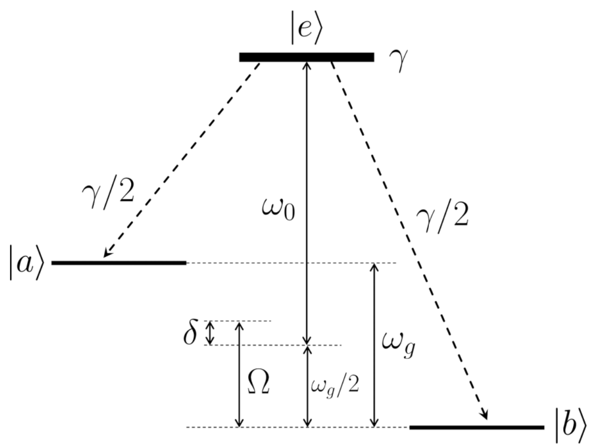

FIG. 1. The energy level diagram under consideration.

excited-state level $|e\rangle$ should be coupled with the ground ones $|a\rangle$ and $|b\rangle$, which we considered here as nondegenerate, $\omega_a - \omega_b = \omega_g$; see Fig. 1. In our case the coupling is due to electric-dipole transitions induced by a bichromatic optical field

$$\mathcal{E}(t) = -\tfrac{1}{2}\{\mathcal{E}_{-1}e^{-i[(\omega_0-\Omega)t-\varphi(t)]} - \mathcal{E}_1 e^{-i[(\omega_0+\Omega)t+\varphi(t)]}\} + \text{c.c.}, \tag{1}$$

where $\varphi(t) = m \sin\omega_m t$ is the modulation needed for producing in-phase and quadrature signals. The frequency ω_0 is taken to be equal to a half sum of the involved transitions, wherein $\omega_0 \gg \omega_g$, i.e., the long- and short-wavelength spectral components are resonant to the transitions $|a\rangle \to |e\rangle$ and $|b\rangle \to |e\rangle$, correspondingly. The dipole moments of both transitions are taken equal and real. The frequency Ω is close to $\omega_g/2$, and the difference gives two-photon detuning δ.

It is known [18] that we can arrive at the following set of equations for the density-matrix elements using the rotating-wave approximation, assuming a low saturation regime and adiabatically eliminating the excited state [19]:

$$\rho_{ee} = \frac{2}{\gamma\Gamma}\{V_{-1}^2\rho_{aa} + V_1^2\rho_{bb} - 2V_{-1}V_1\mathrm{Re}[\tilde{\rho}_{ab}(t)]\}, \tag{2a}$$

$$\left[i\frac{\partial}{\partial t} + 2(\tilde{\delta} + m\omega_m\cos\omega_m t) + i\tilde{\Gamma}_g\right]\tilde{\rho}_{ab} = i\frac{V_{-1}V_1}{\Gamma}. \tag{2b}$$

In the equations above, we imply for the Rabi frequencies that $V_{-1} = d\mathcal{E}_{-1}/2\hbar = V_1 = d\mathcal{E}_1/2\hbar = V$ and $\rho_{aa} = \rho_{bb} \simeq 1/2$, but retain the lower indices for convenience, and γ and Γ are the decay rates of the excited-state population and of the optical coherences, respectively. The ground-state relaxation rate $\tilde{\Gamma}_g = \Gamma_g + (V_{-1}^2 + V_1^2)/\Gamma$ accounts for the resonance power broadening. The light shift δ_0 can be accounted in detuning $\tilde{\delta} = \delta - \delta_0$, but it is not the object of our interest here. Finally, we specially note that $\tilde{\rho}_{ab}$ is not the coherence itself, but its slowly varying amplitude: $\rho_{ab} = \tilde{\rho}_{ab}e^{-2i\Omega t}$.

Equation (2b) can be straightforwardly integrated or be solved numerically. However, these approaches do not give an understanding about the influence of the modulation on the CPT resonance structure. Instead, we will use the replacement $\tilde{\rho}_{ab} \to \bar{\rho}_{ab}e^{2im\sin\omega_m t}$ to make as a step behind in the derivation of the equations. This gives

$$\rho_{ee} = \frac{2}{\gamma\Gamma}\{V_{-1}^2\rho_{aa} + V_1^2\rho_{bb} - 2V_{-1}V_1\mathrm{Re}[e^{2im\sin\omega_m t}\bar{\rho}_{ab}(t)]\}, \tag{3a}$$

$$\left(i\frac{\partial}{\partial t} + 2\tilde{\delta} + i\tilde{\Gamma}_g\right)\bar{\rho}_{ab} = i\frac{V_{-1}V_1}{\Gamma}e^{-2im\sin\omega_m t}. \tag{3b}$$

The equations above now can be directly treated via the Fourier series expansion of $\bar{\rho}_{ab}$ over the frequency ω_m and the Jacobi-Anger one for $e^{\mp 2im\sin\omega_m t}$. At first, for the amplitude of the zeroth harmonic A_0 of ρ_{ee} over ω_m, which determines the nonoscillating part of the optical field transmission studied in the experiment, we have

$$A_0 = \frac{V^2}{\gamma\Gamma}\left[1 - 2\tilde{\Gamma}_g\frac{V^2}{\Gamma}\sum_{k=-\infty}^{\infty}\frac{J_k^2(2m)}{(2\tilde{\delta} + k\omega_m)^2 + \tilde{\Gamma}_g^2}\right], \tag{4}$$

where we used the relations $V_{-1} = V_1$ and $\rho_{aa} = \rho_{bb} = 1/2$, and $J_k(\cdot)$ is the Bessel function of the first kind of the index k. The amplitude A_0 can be obtained from the absorption signal by averaging over $T = 2\pi/\omega_m$ due to the orthogonality property of the trigonometric functions.

Equation (4) demonstrates that the modulation provides a multipeak structure of the CPT resonance, which becomes resolved with growth of ω_m; see Fig. 3. This feature can be understood as follows. In contrast to the standard situation, the optical field prepares the ground-state coherence not only at the frequency 2Ω (difference of resonant spectral component frequencies), but also at frequencies $2\Omega + k\omega_m$. When $2\Omega + k\omega_m = \omega_g$, the amplitude of the corresponding oscillations of the ground-state coherence reaches maxima providing minimum in the absorption for the probing process.

Considering the in-phase and quadrature signals, their shape can be relatively complicated at moderate values of m and ω_m. This feature also stems from the fact that they have a multicomponent structure. For example, the amplitude of the quadrature signal A_Q is determined by the function

$$A_Q \propto \sum_{k=-\infty}^{\infty}(2\bar{\delta} + k\bar{\omega}_m)\frac{J_k(2m)[J_{k-1}(2m) - J_{k+1}(2m)]}{(2\bar{\delta} + k\bar{\omega}_m)^2 + 1}, \tag{5}$$

where $\bar{\delta} = \tilde{\delta}/\tilde{\Gamma}_g$, and $\bar{\omega}_m = \omega_m/\tilde{\Gamma}_g$ (the parameters are normalized on the ground-state coherence relaxation rate), which demonstrates that there are dispersive-shaped curves that have a zero-crossing point at frequencies corresponding to the peaks in the mean in time absorption; see Fig. 4.

There are oscillations of ρ_{ee} not only at frequency ω_m, but also at its multiples, $k\omega_m$. They can be understand as a result of probing the coherence oscillations at frequency $2\Omega + s\omega_m$ by the product of the optical field's components oscillating at frequencies $2\Omega + s\omega_m \mp k\omega_m$. Therefore, for example, there are terms $\propto J_k(2m)J_{k-1}(2m)$, $\propto J_k(2m)J_{k+1}(2m)$ in Eq. (5). Similarly, the expression determining the oscillations of ρ_{ee} at $2\omega_m$ will contain products $J_k(2m)J_{k-2}(2m)$ and $J_k(2m)J_{k+2}(2m)$, etc.

Finally, when $V_{-1} \neq V_1$, and the frequencies of the spectral components are detuned from the transitions $|a\rangle \to |e\rangle$, $|b\rangle \to |e\rangle$, the CPT resonance becomes asymmetric and the side peaks of A_0 pull the frequency of the central one. A

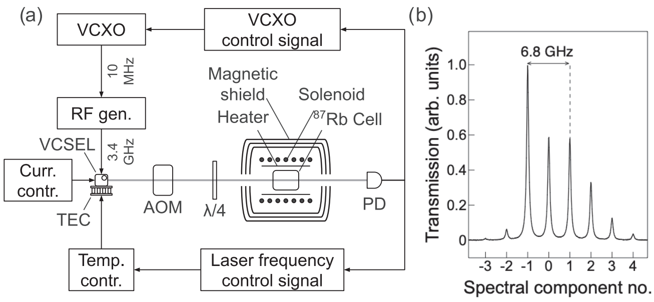

FIG. 2. (a) Scheme of the experimental setup. TEC—thermoelectric cooler; PD—photodetector; AOM—acousto-optic modulator. (b) Spectrum of the laser radiation used in the experiment.

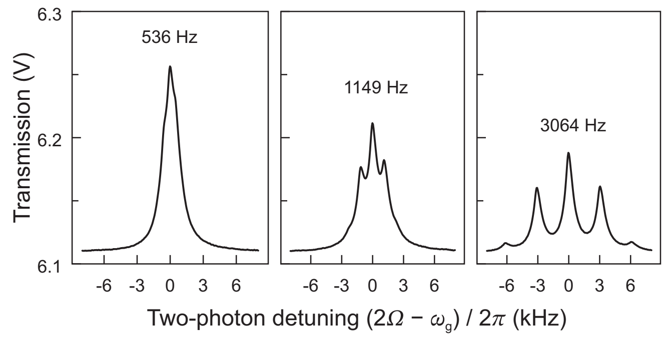

FIG. 3. Multipeak structure of the CPT resonance (nonoscillating part of the laser field transmission) observed experimentally at $\omega_m/2\pi$ equal to 536, 1149, and 3064 Hz. The modulation index m was fixed and equal to 0.65.

similar situation occurs for the in-phase and quadrature signals. Since in the case of bichromatic optical field with different powers of spectral components $\rho_{aa} \neq \rho_{bb}$, equations for the ground-state populations are required to describe the CPT resonance. Fourier amplitudes of the coherence and populations are coupled and there is no general analytical solution of the equations. However, for $m \ll 1$, the expressions describing the frequency shifts of the signals can be obtained [16]. Specifically, for the zero-crossing point of the sum of signals, we have the following shift:

$$\delta_{as} \propto \frac{V_{-1}^2 - V_1^2}{\Gamma} \frac{(1+\bar{\omega}_m)(1+\bar{\omega}_m^2)}{1+\bar{\omega}_m(3+\bar{\omega}_m^2)}. \tag{6}$$

This function falls with growth of $\bar{\omega}_m$ from the zero, reaches a minimum at $\bar{\omega}_m \simeq 0.47$, and after that grows. For $\bar{\omega}_m \gg 1$ the shift has the same value as for $\bar{\omega}_m \ll 1$, i.e., this function demonstrates a behavior typical for the frequency pulling. Also, δ_{as} linearly depends on the optical field intensity in these cases since it is proportional to $(V_{-1}^2 - V_1^2)/\Gamma$. In contrast, δ_{as} is a nonlinear function of the optical field intensity at moderate values of $\bar{\omega}_m$ as far as $\tilde{\Gamma}_g$ contains the power broadening.

III. EXPERIMENT

The experimental setup is schematically shown in Fig. 2(a). We used a single-mode vertical-cavity surface-emitting laser (VCSEL) generating at ≃795 nm. The dc and rf components of the injection current were fed to the laser via a bias tee. The modulation frequency $\Omega/2\pi$ was close to 3.417 GHz, and the first-order sidebands of the polychromatic optical field were tuned to transitions $F_g = 2 \rightarrow F_e = 2, F_g = 1 \rightarrow F_e = 2$ of the ^{87}Rb D_1 line. The power of the rf field and the injection current value were set to provide a significant difference between the powers of the resonant spectral components [see the inset in Fig. 2(b)] and cause a noticeable asymmetry of the CPT resonance. A quarter-wave plate was used to form the CPT resonance in the σ^+-σ^+ scheme. The diameter of the laser beam was 3 mm. The laser wavelength was stabilized by a feedback loop that controls the temperature of the laser diode.

A cylindrical atomic cell (8 mm diameter, 15 mm length, 0.7 mm wall thickness) filled with isotopically enriched ^{87}Rb and Ne at a pressure of 90 Torr was under study. The atomic cell was placed in a longitudinal magnetic field of 0.02 G to separate the metrological microwave transition from the magnetosensitive ones at sublevels $m_{F_g} = \pm 1$. The temperature of the atomic cell was maintained close to 65 °C with an accuracy of 0.01 °C. The cell, the heater, and the solenoid were placed in a three-layer μ-metal magnetic shield, providing an over 500-fold suppression of the laboratory magnetic field.

To stabilize the frequency of the voltage-controlled crystal oscillator (VCXO), which served as a local oscillator, the rf signal frequency was modulated: $j(t) = j_{dc} + j_{rf}\cos(\Omega t + m \sin \omega_m t)$. Figure 3 shows the experimentally registered nonoscillating part of the CPT resonance. The rf frequency was scanned at a rate of 1 kHz/s around 3.417 359 GHz. The signal of the cell transmission was low-pass filtered ($f_c = 10$ Hz) and averaged over five scans. The laser radiation power was 60 μW. Figure 3 demonstrates the evolution of the laser field transmission with the growth of the modulation frequency ω_m while maintaining the modulation index $m = 0.65$. When the value of ω_m exceeds the ground-state relaxation rate, the multipeak structure becomes resolved. Experimentally, for a modulation frequency $\omega_m/2\pi = 3064$ Hz we clearly observed five separated peaks with a width of about 950 Hz. The amplitudes A_k of the registered peaks are determined by the squares of the Bessel functions of the corresponding index: for the central peak $A_0 \propto J_0^2(2m)$, for the first side peaks $A_{\pm 1} \propto J_1^2(2m)$, etc., as follows from Eq. (4). It can be seen that all peaks have the same type of asymmetry: The left slope is steeper than the right. Therefore, the frequency of the central peak is pulled.

To obtain the error signal, the transmission signal of the atomic cell was demodulated at a frequency of $\omega_m/2\pi$ using a lock-in amplifier. The experimentally obtained error signal for the modulation frequency $\omega_m/2\pi$, approximated by the theoretical curve, is shown in Fig. 4(a). An excellent agreement between the theory and experimental data can be seen. Figure 4(b) demonstrates that due to the multipeak structure of the resonance, the error signal is the sum of the dispersion curves from each peak, which explains its rather complex shape.

Figure 5 shows the dependence of the CPT resonance frequency on ω_m for a fixed value of $m = 0.65$. The VCXO frequency was stabilized at a value corresponding to the zero-crossing point of the error signal and was measured with a

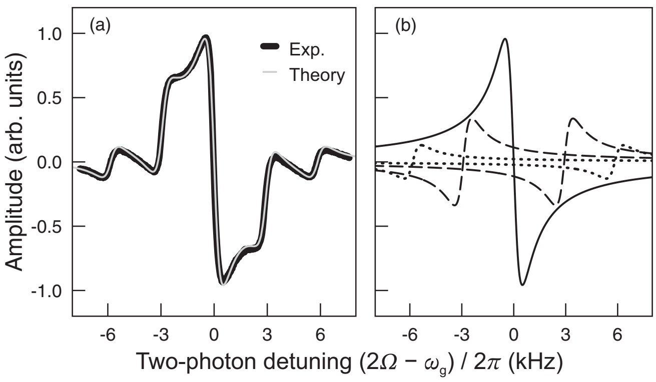

FIG. 4. (a) Quadrature signal for $\omega_m/2\pi = 3064$ Hz, $m = 0.65$, and theoretical fit made via Eq. (5) for $\tilde{\Gamma}_g/2\pi = 480$ Hz. (b) Individual components of the error signal plotted according to terms in the sum of Eq. (5). The solid line is for $k = 0$, and the dashed and dotted lines are for $k = \pm 1$ and $k = \pm 2$, correspondingly.

frequency counter referenced to a passive H maser. When the modulation frequency is smaller than the individual width of the peaks, the in-phase signal has a steeper slope than the quadrature signal. In the opposite case the steepness of the in-phase signal drops and the quadrature signal dominates. For each value of ω_m, the phase of synchronous detection was set to maximize the slope, therefore a mixture of in-phase and quadrature signals was used as the error signal. The initial increase of the frequency at small values of ω_m is associated with pulling of the central peak towards the high-frequency side peaks. The maximum shift of the error-signal frequency, caused by the pulling effect, reaches a value of 14 Hz, which is quite large while the error signal in Fig. 4 looks symmetric. It is achieved at $\omega_m/2\pi \simeq 460$ Hz, which is close to the half width of the CPT resonance for $m = 0$ and is in good agreement with the theoretical prediction. At modulation frequencies significantly higher than the widths of the peaks the effect of frequency pulling is small.

We obtained the dependencies of the CPT resonance frequency on the optical field power for two cases: when the pulling is present ($\omega_m/2\pi = 230$ Hz) and when it is suppressed ($\omega_m/2\pi = 10$ kHz) [Fig. 6(a)]. The first case corresponds to a point on the left slope of the dependence shown in Fig. 5. The VCXO frequency was stabilized and measured in the same way as described above, while the laser power was linearly varied using an acousto-optic modulator. The increase in resonance frequency with power is mainly caused by the light shift. The difference between the two dependences is due to the frequency pulling which gives a shift of the order of 10 Hz nonlinearly dependent on the optical field intensity. The transition to high values of ω_m provides a significant reduction of δ_{as}, and its nonlinear part $\approx$2 Hz; see Fig. 6(b). This residual shift was obtained by subtracting the linear fit from the experimental data.

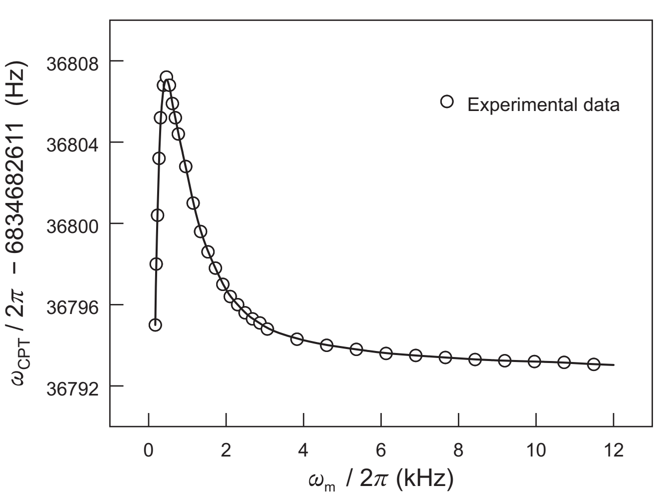

FIG. 5. The dependence of the CPT resonance frequency on the modulation frequency. Circles are experimental data, and the solid line is a guide for the eyes.

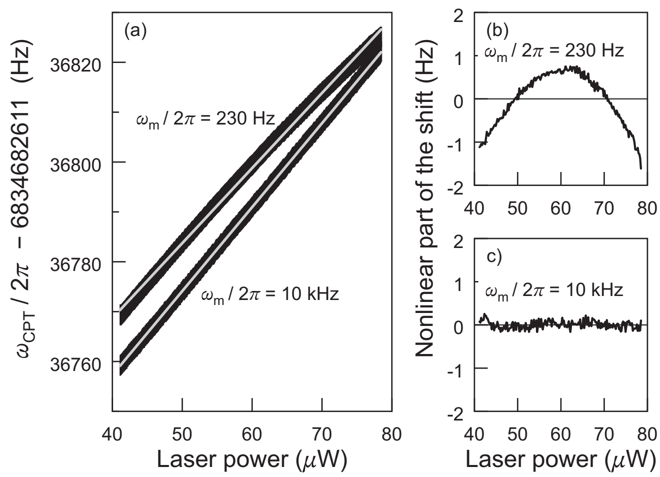

FIG. 6. (a) The dependence of the CPT resonance frequency on the laser power for two modulation frequencies. Gray lines are the linear approximation. (b) and (c) Nonlinear parts of the curves shown in (a).

IV. DISCUSSION

Our theoretical calculations show that the slope of the error signal in the case of high modulation frequencies ω_m is approximately 1.21 times smaller compared to the mixture of in-phase and quadrature signals having maximal possible steepness. However, the use of high-frequency modulation has some advantages besides suppressing the shift δ_{as}, that occurs due to the frequency pulling effect. First, it can be more beneficial due to the decreased level of low-frequency noise. The second advantage is the simplicity of finding the maximal slope of the central dispersive curve. It is determined by the product $J_0(2m)J_1(2m)$; see Eq. (5). Therefore, only the value of the modulation index m should be set to 0.54. In contrast, in a moderate-frequency regime (compared to the width of the peaks), the ratio of ω_m to the ground-state relaxation rate and the phase of synchronous detection must also be optimized.

The inequality in the powers of the resonant components is considered to be the main source of the CPT resonance asymmetry. But, in principle, the spectrum can be made symmetrical. For example, we have recently demonstrated that the powers of the first-order sidebands can be equalized by an additional modulation of the injection current at a doubled microwave frequency [20]. However, there are other sources of the resonance asymmetry: the inequality of populations of working sublevels due to unequal spontaneous transitions from the excited state to the ground one [21], inhomogeneity of the magnetic field, the temperature gradient in the atomic cell [22], transverse inhomogeneity of the laser beam when the light shift is unsuppressed [23,24], and the optical field absorption [16]. Therefore, we generalize results of Ref. [17]: The use of high modulation frequency ω_m should suppress the frequency pulling due to all the above-mentioned sources.

V. SUMMARY

We have considered a situation where the phase modulation is used to stabilize a local oscillator frequency in chip-scale atomic clocks. In this case, the CPT resonance consists of several peaks pulling the frequency of the central one if the resonance is asymmetric. The pulling drops off when peaks are resolved, i.e., when the modulation frequency significantly exceeds the relaxation rate of the ground-state coherence.

For each peak in the optical field transmission, there is a dispersive-shape curve in the quadrature signal, i.e., it has a multidispersive structure. The central curve is also affected by the frequency pulling. As we have demonstrated, the dependence of its frequency on ω_m vanishes when the curves become resolved. Finally, we have obtained a linear dependence of the quadrature signal frequency when the pulling is suppressed.

[1] J. Kitching, Appl. Phys. Rev. **5**, 031302 (2018).

[2] S. Knappe, V. Velichansky, H. G. Robinson, L. Liew, J. Moreland, J. Kitching, and L. Hollberg, Atomic vapor cells for miniature frequency references, in *Proceedings of the IEEE International Frequency Control Symposium and PDA Exhibition Jointly with the 17th European Frequency and Time Forum* (IEEE, New York, 2003), pp. 31 and 32.

[3] S. Knappe, V. Gerginov, P. Schwindt, V. Shah, H. Robinson, L. Hollberg, and J. Kitching, Opt. Lett. **30**, 2351 (2005).

[4] I. Ben-Aroya, M. Kahanov, and G. Eisenstein, Opt. Express **15**, 15060 (2007).

[5] M. Kahanov, I. Ben-Aroya, and G. Eisenstein, Opt. Lett. **33**, 944 (2008).

[6] S. Knappe, R. Wynands, J. Kitching, H. G. Robinson, and L. Hollberg, J. Opt. Soc. Am. B **18**, 1545 (2001).

[7] J. Vanier, Appl. Phys. B **81**, 421 (2005).

[8] V. Gerginov, S. Knappe, V. Shah, P. D. D. Schwindt, L. Hollberg, and J. Kitching, J. Opt. Soc. Am. B **23**, 593 (2006).

[9] V. Shah and J. Kitching, Advances in coherent population trapping for atomic clocks, in *Advances in Atomic, Molecular, and Optical Physics*, edited by E. Arimondo, P. Berman, and C. Lin (Academic Press, San Diego, 2010), Vol. 59, Chap. 2, pp. 21–74.

[10] A. Godone, F. Levi, C. E. Calosso, and S. Micalizio, Nuovo Cimento Riv. Ser. **38**, 133 (2015).

[11] F. Levi, A. Godone, and J. Vanier, IEEE T-UFFC **47**, 466 (2000).

[12] M. Zhu and L. S. Cutler, Theoretical and experimental study of light shift in a CPT-based Rb vapor cell frequency standard, in *Proceedings of 32nd Annual Precise Time and Time Interval (PTTI) Meeting*, edited by L. A. Breakiron (United States Naval Observatory, Washington, DC, 2001), pp. 311–324.

[13] V. Shah, V. Gerginov, P. D. D. Schwindt, S. Knappe, L. Hollberg, and J. Kitching, Appl. Phys. Lett. **89**, 151124 (2006).

[14] M. I. Vaskovskaya, E. A. Tsygankov, D. S. Chuchelov, S. A. Zibrov, V. V. Vassiliev, and V. L. Velichansky, Opt. Express **27**, 35856 (2019).

[15] E. A. Tsygankov, S. A. Zibrov, M. I. Vaskovskaya, D. S. Chuchelov, V. V. Vassiliev, V. L. Velichansky, A. E. Drakin, and A. P. Bogatov, Opt. Express **30**, 2748 (2022).

[16] E. A. Tsygankov, S. V. Petropavlovsky, M. I. Vaskovskaya, D. S. Chuchelov, S. A. Zibrov, V. V. Vassiliev, V. L. Velichansky, and V. P. Yakovlev, arXiv:2012.13731.

[17] V. Yudin, M. Y. Basalaev, A. Taichenachev, O. Prudnikov, D. Radnatarov, S. Kobtsev, S. Ignatovich, and M. Skvortsov, Phys. Rev. A **108**, 013103 (2023).

[18] D. S. Chuchelov, V. V. Vassiliev, M. I. Vaskovskaya, V. L. Velichansky, E. A. Tsygankov, S. A. Zibrov, S. V. Petropavlovsky, and V. P. Yakovlev, Phys. Scr. **93**, 114002 (2018).

[19] D. Chuchelov, E. Tsygankov, S. Zibrov, M. Vaskovskaya, V. Vassiliev, A. Zibrov, V. Yudin, A. Taichenachev, and V. Velichansky, J. Appl. Phys. **126**, 054503 (2019).

[20] A. P. Bogatov, A. E. Drakin, M. I. Vaskovskaya, D. S. Chuchelov, K. M. Sabakar, E. A. Tsygankov, V. V. Vassiliev, V. L. Velichansky, and S. A. Zibrov, Opt. Lett. **47**, 6425 (2022).

[21] K. M. Sabakar, M. I. Vaskovskaya, D. S. Chuchelov, E. A. Tsygankov, V. V. Vassiliev, S. A. Zibrov, and V. L. Velichansky, Phys. Rev. Appl. **20**, 034015 (2023).

[22] P. J. Oreto, Y.-Y. Jau, A. B. Post, N. N. Kuzma, and W. Happer, Phys. Rev. A **69**, 042716 (2004).

[23] J. C. Camparo, R. P. Frueholz, and C. H. Volk, Phys. Rev. A **27**, 1914 (1983).

[24] D. S. Chuchelov, E. Tsygankov, M. L. Vaskovskaya, S. A. Zibrov, V. E. Velichansky, S. V. Petropavlovsky, and V. P. Yakovlev, J. Phys.: Conf. Ser. **1686**, 012029 (2020).